BIOCHEMISTRY
including biophysical chemistry & molecular biology

Article

pubs.acs.org/biochemistry

Hydrogen Exchange Differences between Chemoreceptor Signaling Complexes Localize to Functionally Important Subdomains

Seena S. Koshy,[†] Xuni Li,[†] Stephen J. Eyles,[‡] Robert M. Weis,[†,§,∥] and Lynmarie K. Thompson*[,†,§]

[†]Department of Chemistry, [‡]Department of Biochemistry and Molecular Biology, and [§]Program in Molecular and Cellular Biology, University of Massachusetts, Amherst, Massachusetts 01003, United States

Supporting Information

ABSTRACT: The goal of understanding mechanisms of transmembrane signaling, one of many key life processes mediated by membrane proteins, has motivated numerous studies of bacterial chemotaxis receptors. Ligand binding to the receptor causes a piston motion of an α helix in the periplasmic and transmembrane domains, but it is unclear how the signal is then propagated through the cytoplasmic domain to control the activity of the associated kinase CheA. Recent proposals suggest that signaling in the cytoplasmic domain involves opposing changes in dynamics in different subdomains. However, it has been difficult to measure dynamics within the functional system, consisting of extended arrays of receptor complexes with two other proteins, CheA and CheW. We have combined hydrogen exchange mass spectrometry with vesicle template assembly of functional complexes of the receptor cytoplasmic domain to reveal that there are significant signaling-associated changes in exchange, and these changes localize to key regions of the receptor involved in the excitation and adaptation responses. The methylation subdomain exhibits complex changes that include slower hydrogen exchange in complexes in a kinase-activating state, which may be partially consistent with proposals that this subdomain is stabilized in this state. The signaling subdomain exhibits significant protection from hydrogen exchange in complexes in a kinase-activating state, suggesting a tighter and/or larger interaction interface with CheA and CheW in this state. These first measurements of the stability of protein subdomains within functional signaling complexes demonstrate the promise of this approach for measuring functionally important protein dynamics within the various physiologically relevant states of multiprotein complexes.

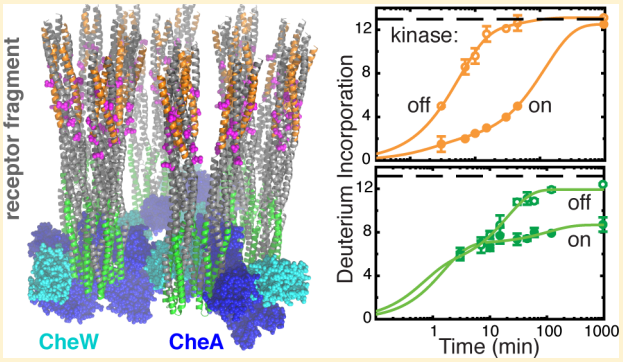

Membrane proteins perform key life processes, including transmitting information into cells to allow responses to the environment. Bacterial chemotaxis receptors make up an ideal system for investigations of the mechanistic details of transmembrane signaling. Bacteria sense chemicals in the environment and relay a signal through the chemoreceptors that ultimately controls the swimming response of the cell. The membrane-spanning receptors form ternary complexes (Figure 1A) with two cytoplasmic proteins, a scaffolding protein CheW and a histidine kinase CheA; these complexes are found in large hexagonal arrays primarily at the poles of the cell. On the basis of a wide variety of studies, including Cys cross-linking, mutagenesis, electron paramagnetic resonance (EPR), and solid-state nuclear magnetic resonance, ligand binding to the receptor is thought to cause an ~2 Å piston motion of an α helix in the periplasmic and transmembrane domains.[1] It is less clear how the signal is then propagated through the cytoplasmic domain to inhibit the kinase bound ~200 Å away at the membrane-distal tip of the receptor, and how methylation of Glu residues in this domain restores kinase activation as part of receptor adaptation to ongoing stimuli.

A number of studies have suggested that changes in dynamics in the cytoplasmic domain may play a role in signaling, but it is difficult to measure dynamics within membrane proteins and large functional multiprotein complexes. Previous studies from our laboratory have shown that the cytoplasmic fragment is highly dynamic in solution,[2] and small changes (mutation of a single residue or protonation of a few residues) can lead to significant stabilization of a large fraction of the protein.[3] Proposals that receptor signaling involves changes in dynamics[3,4] have been corroborated by mutagenesis and cross-linking results. For example, electrostatic interactions are thought to affect the conformational dynamics of the methylation subdomain, with charge-neutralizing mutations at the acidic methylation sites and other sites favoring a less dynamic, kinase-activating state.[5] On the basis of cysteine cross-linking and alanine knob mutational studies, Falke and co-workers have recently proposed that signaling involves antisymmetric changes in dynamics in different subdomains of the cytoplasmic domain: the kinase-inhibited state is proposed to be destabilized in the methylation subdomain

Received: May 28, 2014
Revised: November 24, 2014
Published: November 24, 2014

   dx.doi.org/10.1021/bi500657v | *Biochemistry* 2014, 53, 7755−7764

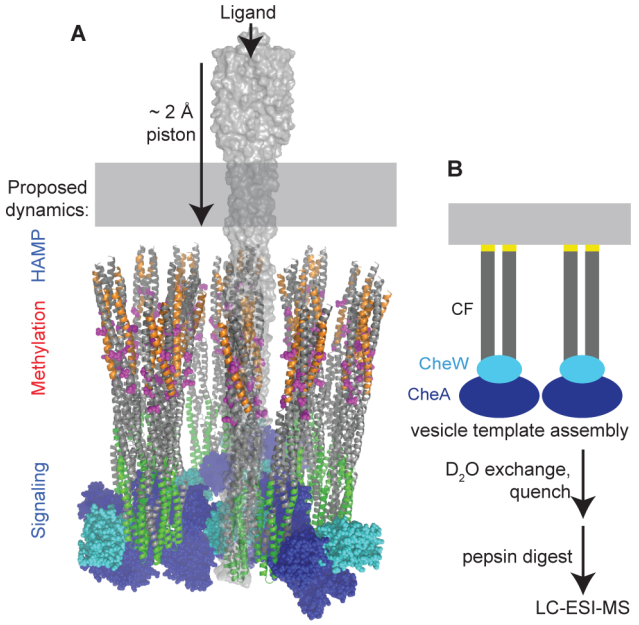

Figure 1. HDX-MS approach for testing proposed changes in dynamics of chemoreceptors within functional complexes during signaling. (A) Model of a single-transmembrane chemoreceptor dimer (gray surface) superimposed on one cytoplasmic fragment dimer within a model of signaling complexes with CheW (cyan) and CheA (blue) in the receptor array (coordinates kindly provided by B. Crane). One hexagon of the array model is shown, containing six trimers of receptor cytoplasmic fragment dimers, with magenta indicating receptor methylation sites. Note that all 18 receptor dimers extend through the membrane, but only a single intact receptor dimer (gray surface model) is shown for the sake of clarity. Ligand inhibition of the CheA kinase begins with a piston motion of an α helix in the periplasmic and transmembrane domains. This has been proposed to cause the changes in dynamics listed at the left, with blue representing decreased dynamics in the HAMP and signaling subdomains and red representing increased dynamics in the methylation subdomain. Note that the array model does not include the HAMP subdomain, because it is not present in the CF construct used in this study. (B) HDX-MS method for measurement of dynamics in functional complexes of receptor cytoplasmic fragments that contain His tags (yellow) that mediate binding to vesicles for assembly of complexes. Assembled complexes were exchanged in D_2O for various times before quenching, pepsin digestion, and analysis by LC−ESI-MS. HDX-MS measurements reported here demonstrate that a kinase-inhibited state has increased exchange rates in peptides of the methylation subdomain (orange on the array model) and decreased levels of protection in peptides of the signaling subdomain (green on the array model).

and stabilized in the signaling subdomain that interacts with CheA and CheW, relative to the kinase-activating state.[6] Also on the basis of mutagenesis studies, Parkinson and co-workers have proposed a compatible model involving changes in dynamics in which the kinase-inhibited state again has a destabilized methylation subdomain and also has a stabilized HAMP subdomain.[7] What has been lacking until now is a means for direct measurement of dynamics in functional receptor complexes to test these proposals (listed in Figure 1A, left) and delineate the role of changing dynamics in the signaling mechanism.

There has been tremendous recent progress in mass spectrometry of membrane proteins,[8,9] including hydrogen exchange mass spectrometry (HDX-MS) studies of dynamics of membrane proteins in detergent micelles[10−15] and nanodiscs.[16] We have developed an alternate approach, summarized in Figure 1B, that can be applied for HDX-MS studies of a soluble domain of a membrane protein in membrane-bound functional complexes with its partner proteins. We have shown that vesicle template assembly can be combined with HDX-MS to measure dynamics in membrane-bound functional complexes.[17] The vesicle template assembly method[18] employs vesicles containing a nickel-chelating lipid to bind a His-tagged chemoreceptor cytoplasmic fragment (CF) and assemble functional complexes with CheA and CheW in different signaling states.[19] The potential generality of this assembly method has been demonstrated by its use to assemble functional complexes of other systems such as eukaryotic receptor tyrosine kinases.[20−23] With HDX-MS, we have demonstrated that the rapid global hydrogen exchange rates (exchange throughout the entire protein) observed for the Asp receptor CF in solution are reduced by assembly of functional CF complexes, but there are no large changes in CF global exchange rates between samples representative of different signaling states.[17] Here we report measurements of local exchange in functional CF complexes that mimic two signaling states. Functional complexes are exchanged in D_2O for various times before quenching at low pH, pepsin digestion, and analysis by LC−ESI-MS. This localizes the exchange information to the individual peptide products of the pepsin digest. Our data show that stabilization of the CF upon formation of functional complexes extends throughout most of the protein, but that changes in dynamics between complexes that mimic the signaling states localize to key regions of the receptor critical to excitation (control of the CheA kinase) and adaptation (mediated by methylation of specific Glu residues). In both subdomains, there is some reduction in the exchange rate in the kinase-activating state, which suggests that the mechanism of kinase activation involves stabilization of two key features of the chemoreceptor, its methylation subdomain involved in adaptation and its interactions between the signaling subdomain and CheA and CheW involved in kinase activation in the signaling array. These changes are measured within arrays that are nativelike, with ∼100 nm dimensions[24] and 12 nm hexagonal spacing,[25] comparable to array properties observed in cells. These results illustrate the promise of combining HDX-MS with vesicle template assembly to reveal differences in structure and dynamics between physiologically relevant states of membrane-bound multiprotein complexes and gain insights into the role of dynamics in mechanisms of complex systems.

MATERIALS AND METHODS

Proteins were purified according to published protocols.[24,26−28] Vesicles consisting of mixtures of DOPC and DGS-NTA-Ni^{2+} were extruded and used for vesicle template assembly of functional complexes as previously described,[19] except that excess CheA and CheW were used to drive all of the CF into complexes, as judged by maximizing the kinase activity under high-density conditions after overnight incubation.[28] Functional complexes of 30 μM His-tagged CF_{4E}, 6 μM CheA, and 12 μM CheW with lipid vesicles were assembled at 25 °C in kinase buffer [75 mM Tris, 100 mM KCl, 5 mM $MgCl_2$, 2 mM TCEP, and 5% DMSO (pH 7.5)]. For high-density complexes, 580 μM total lipids were used, with 50% nickel-chelating lipid (290 μM DGS-NTA) and the remainder DOPC. For low-density complexes, 2900 μM total lipids were used, with 10% nickel-chelating lipid (290 μM DGS-NTA) and the remainder DOPC.

dx.doi.org/10.1021/bi500657v | Biochemistry 2014, 53, 7755−7764

Protein binding and kinase activity were measured in all cases to ensure successful formation of functional complexes.

Preparation of exchanged samples and MS analysis was conducted as previously described.[17] A spin column was used to accomplish transfer into deuterated buffer in ~2.5 min, while avoiding dilution of the complex that could lead to protein dissociation during the hydrogen exchange time course. To initiate hydrogen exchange, 1 mL of the assembled complex was applied to a 2 mL G10 Sephadex Zeba desalting column (Pierce Biotechnology) pre-equilibrated with a D_2O kinase buffer at 25 °C. After centrifugation (2000 rpm for 2 min at 25 °C in a Beckman Coulter Allegra 6R Tabletop Centrifuge), complexes were incubated in a 25 °C water bath for deuterium exchange. After exchange times ranging from 30 s longer (3 min total) to 16 h, 30 μL aliquots of the exchanged complex were removed and added to 15 μL of quench buffer [1% formic acid, 20% glycerol, and 1 M GuHCl (pH 1.6)] in a 0 °C water bath, to reach a final pH of 2.5. Our previous global exchange study showed that pH 2.5 quench conditions dissociated 70−80% of CF from vesicles and also caused precipitation of CheA and CheW.[17] Quenched samples were immediately flash-frozen in liquid nitrogen and stored at −80 °C. Immediately prior to MS analysis, each sample was thawed for 3 min in an ice−water bath, digested for 1 min with a 1:1 pepsin/CF mixture, and then analyzed by LC−ESI-MS on a QSTAR-XL hybrid quadrupole/time-of-flight mass spectrometer (AB SCIEX) in positive ion mode at the UMass Mass Spectrometry Center. Samples were injected at a rate of 200 μL/min into the chilled C18 reverse phase column (Higgins Analytical) pre-equilibrated in 95% buffer A (0.1% formic acid in water) and 5% buffer B (0.1% formic acid in acetonitrile). Peptides were eluted into the mass spectrometer with a gradient from 5 to 40% (v/v) buffer B over 4 min, 40% buffer B for 2 min, and then 60% buffer B for 1 min. Preparation of the next sample consisted of equilibration in 95% buffer A and 5% buffer B for 8 min. The thawing, digestion, and HPLC were conducted at 0 °C to minimize back exchange. Between each HPLC injection, a blank sample was injected to ensure there was no carryover of peptides into the subsequent injection.[29] Also, after every five injections, the column was disconnected from the mass spectrometer and washed with 100% buffer B for 30 min to prevent accumulation of lipids in the column. Peptides were previously identified by tandem MS.[17]

Peptides from a D_2O-denatured CF control sample provided values for 100% exchange that were used to calculate percentage deuterium exchange. CF was exchanged using a spin column (2 mL G10 Sephadex Zeba desalting column) into D_2O renaturation buffer [20 mM potassium phosphate (pD 7.5), 50 mM NaCl, and 5% DMSO] and then incubated at 80 °C for 1 h to thermally denature the protein. This renaturation buffer was used because it has been shown[3] to support reversible thermal denaturation of the CF (kinase buffer does not). After cooling for 30 min on ice, the sample was subjected to the protocol described above (quench, freeze, digest, and LC−MS) so that its peptides would undergo equivalent back exchange. Back exchange was computed as the difference between the total exchange observed in peptides derived from the D_2O-denatured CF sample and the maximal possible exchange for each peptide. Back exchange for all the peptides was 20% on average, with a range of 11−31%.[17]

The incorporation of deuterium into each peptide was computed for most cases by measuring the average mass of the isotopic clusters over the full m/z range for the peptide as follows. All of the m/z peaks found in the spectrum between the initial and final exchange cluster positions were selected manually, and a manual reconstruction was done to compute the average molecular weight using Analyst software. The number of incorporated deuterium atoms was then calculated by subtracting the molecular weight of the unexchanged peptide. For all peptides that displayed a significant rapidly exchanging fraction (fully exchanged in 3 min), Gaussian deconvolution was used to estimate this fraction. Analyst software was used to approximate the m/z spectrum by a series of centroid functions (peak position and intensity). The centroid data were analyzed in proFit, by fitting the rapidly exchanging and slower exchanging populations to Gaussian distributions. The amplitude and width of each Gaussian were used to compute its area. The fraction that had fully exchanged did not change significantly at early time points (3, 7, 10, and 15 min). The estimated rapidly exchanging fraction is listed for each peptide in Table S1a of the Supporting Information. For peptides that showed a large (50−75%) rapidly exchanging fraction (orange in Table S1a of the Supporting Information), the average mass method could not be used to measure the exchange of the remaining fraction because the mass would be shifted by the isotopic cluster of the fully exchanged fraction. An alternative method was chosen for a more detailed analysis of the exchange of these peptides (orange peptides in Table S3 of the Supporting Information). The m/z of the most intense peak in the peak cluster corresponding to the fraction not yet fully exchanged was used to compute the average molecular weight. Mass spectra that displayed overlap between the peaks of the two fractions (beginning at 60 or 120 min) were omitted from this analysis.

RESULTS

Hydrogen Exchange Properties of CF Subdomains Differ between Signaling States. Figure 2 shows the structure of a monomer of the Asp receptor CF dimer and the pepsin peptides identified by MS/MS (listed in Tables S1a and S3 of the Supporting Information) that were used to monitor hydrogen exchange. The Asp receptor fragment peptides are represented in the figures within the crystal structure of the 75% identical Ser receptor fragment [Protein Data Bank (PDB) entry 1qu7]. The CF_{4E} construct begins in the methylation subdomain (CF_{4E} is the fully unmethylated state, with glutamic acid at all four methylation sites colored magenta) and lacks the HAMP subdomain that would connect the N-terminus to the transmembrane domain. The signaling subdomain, distal to the membrane, interacts with the CheA kinase and CheW, and the ~30 C-terminal residues serve as a flexible link to the binding site for the CheR methyltransferase. The 26 peptides identified by MS/MS span all of these CF regions, providing overlapping coverage of 87% of the CF sequence.[17]

Hydrogen exchange experiments were performed on complexes of CF_{4E}, CheA, and CheW bound to vesicles under conditions that produce nativelike arrays of CF_{4Q}[25] and also of CF_{4E} (A. Briegel, M. J. Harris, G. J. Jensen, and L. K. Thompson, unpublished results) with activities that mimic the kinase-activating or kinase-inhibited signaling state. Figure 1B summarizes the novel method used to measure hydrogen exchange of functional complexes assembled on vesicles.[17] After rapid transfer of the complex into deuterated buffer using a spin column, hydrogen−deuterium exchange proceeds until it is quenched by decreasing the pH to 2.5 and the temperature to 0 °C. Each sample is flash-frozen and then later thawed for brief

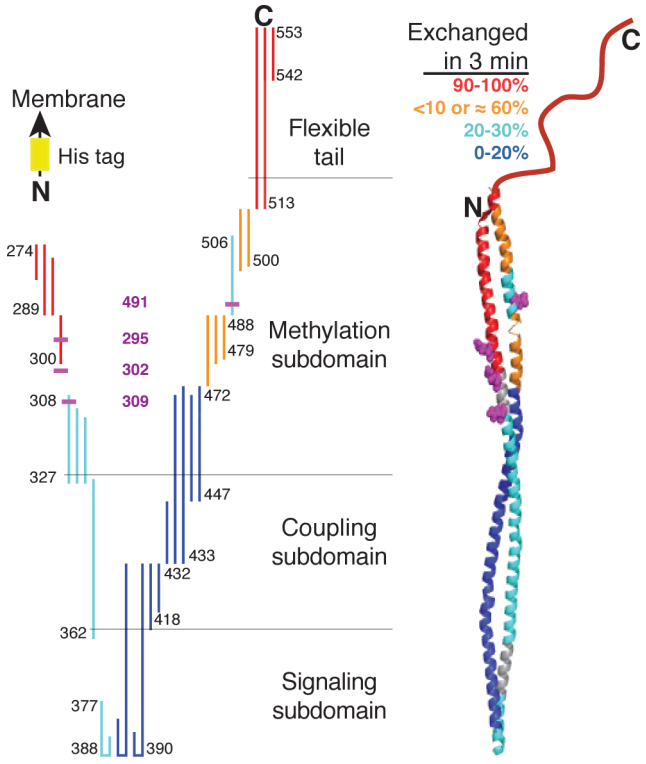

Figure 2. Structure and corresponding peptides of Asp receptor CF_{4E} analyzed in HDX experiments. A monomer model of the CF dimer is shown, based on the Ser receptor CF crystal structure (PDB entry 1qu7) with an additional ~30 amino acids of the receptor on the N-terminus, modeled as an α helix that connects to the rest of the receptor, and ~30 amino acids on the C-terminus as a flexible tail. The four glutamic acid sites that are methylated as part of the adaptation of the receptor to ongoing stimuli are colored magenta with magenta sequence numbers. Peptides identified by MS/MS are labeled with Asp receptor sequence numbers (Ser receptor sequence number minus 2) for the methylation sites and many termini. Both the structure and peptides are colored according to the fraction that is fully exchanged at 3 min, as listed in Table S1b of the Supporting Information. Orange signifies peptides that are <10% fully exchanged at 3 min in the low-density kinase-inhibited state and ~60% fully exchanged at 3 min in the high-density kinase-activating state (see Table S1b of the Supporting Information). Gray signifies regions with no exchange data (no peptide was identified).

(1 min) pepsin proteolysis and analysis of incorporation of deuterium into the resulting peptides by LC−ESI-MS. Thus, exchange occurs in the functional complex, and we have shown there is limited back exchange during subsequent steps before the MS analysis.[17]

We chose to control the signaling state using the density of CF_{4E} assembly on the vesicles, which is determined by the total vesicle surface area containing nickel-chelating lipids that bind the His-tagged CF. The high- and low-density complexes contain similar amounts of CheA and CheW, as previously shown under limiting CheA and CheW conditions[19] and demonstrated in Figure S1 of the Supporting Information for the excess CheA and CheW conditions used here to drive maximal complex formation. High-density CF_{4E} complexes (290 μM nickel-chelating lipid is 50% of the total 580 μM lipid) mimic the kinase-activating state, with high kinase activity and low methylation activity, and low-density CF_{4E} complexes (290 μM nickel-chelating lipid is 10% of the total 2.9 mM lipid) mimic the kinase-inhibited state, with low kinase activity and high methylation activity.[19] Because electron cryotomography[30] and receptor reconstitution studies[31] indicate that receptor arrays do not dissociate during signaling, it seems likely that high-density assembly forces CF_{4E} (a methylation state that does not normally activate the kinase) to pack more closely to mimic the kinase-activating state, consistent with shorter receptor−receptor distances shown by Förster resonance energy transfer for kinase-activating cytoplasmic fragments[19] and for ligand-free intact receptor (corresponding to the kinase-activating state, although the intact receptor samples lacked CheA and CheW).[32] Thus, perhaps ligand inhibition of kinase activity begins with a subtle 2 Å piston in the periplasmic and transmembrane domains that causes a similarly subtle expansion of the cytoplasmic domain, undetectable at the resolution of the electron cryotomography studies.[33] This plausible mechanism and the observation of consistent complex formation and inverse changes in kinase and methylation activity support the use of high- and low-density template-assembled preparations for an initial comparison of the two signaling states. This choice is further supported by the high specific activities of 12−13 s^{-1} (per total CheA, equivalent to 25 s^{-1} for the typical 50% fraction of bound CheA under these conditions) measured for the kinase-activating CF_{4E} complexes.

Figures 2 and 3 and Tables S1 and S2 of the Supporting Information provide an overview of the hydrogen exchange behavior of CF in functional complexes assembled at high and low densities to mimic the signaling states. In Figure 2, the structure and peptides are colored according to the fraction that undergoes complete exchange in 3 min. The red peptides from the N- and C-terminal regions undergo rapid exchange that is complete in 3 min. This behavior is observed for three peptides from the C-terminal tail, consistent with the known flexibility of this segment that tethers the CheR binding site to the receptor.[34] Complete exchange in 3 min is also observed for four N-terminal peptides. This rapid exchange suggests that stability of the CF in this region is compromised, perhaps because of the truncation of the CF from the rest of the receptor.

All of the other peptides exhibit slower exchange, indicating that the reduced level of global exchange we observed in functional complexes[17] extends throughout most of the CF. The small error bars for the exchange data in the tables and figures show the consistency between two independent data sets for each signaling state (Figures 4 and 5 and Figure S1 of the Supporting Information) and between the behavior of overlapping peptides (Tables S1b and S2 of the Supporting Information). The difference in deuterium incorporation levels at various exchange times (Table S2 of the Supporting Information) is represented by the colors in Figure 3. This overview illustrates that this high-density kinase-activating state has (1) increased exchange at 3 min (red), in part because of a fraction that undergoes complete exchange in 3 min, and (2) decreased exchange from 30 min to 16 h (blue, cyan) localized to the methylation and signaling subdomains.

The Methylation Subdomain Exhibits both Increased and Decreased Exchange Rates in a High-Density Kinase-Activating State. Peptides of the methylation subdomain exhibit two distinct differences in exchange behavior in the high- versus low-density signaling states. This is illustrated by the data shown in Figure 4A for a 16-residue peptide (residues 473−488, highlighted in bright orange) and in Figure 4B for a 13-residue peptide (residues 500−512, highlighted in pale orange). The high-density complex exhibits

dx.doi.org/10.1021/bi500657v | Biochemistry 2014, 53, 7755−7764

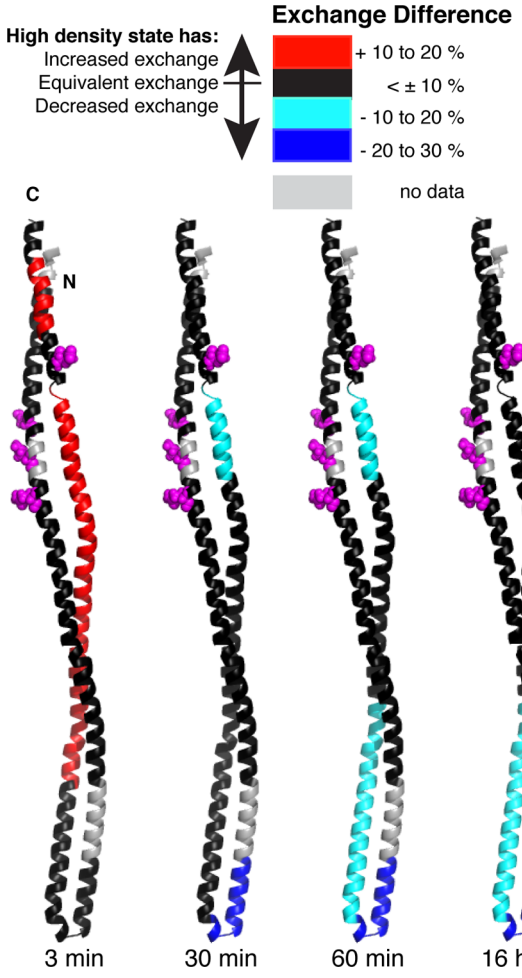

Figure 3. Difference in the time course of deuterium incorporation between high- and low-kinase activity complexes. The monomer of the cytoplasmic fragment dimer structure is shown for the sake of clarity and colored according to the difference in the incorporation of deuterium into CF_{4E} assembled at a high density on 1:1 DGS-NTA-Ni^{2+}/DOPC vesicles (kinase-activating) and CF_{4E} assembled at a low density on 1:9 DGS-NTA-Ni^{2+}/DOPC vesicles (kinase-inhibited). The percent deuterium incorporation was calculated using the average mass method. Data for overlapping peptides were averaged for each state (Table S2 of the Supporting Information) and then subtracted (high density minus low density).

both slower exchange (compare arrows) and a rapidly exchanging fraction with full exchange in 3 min (asterisk). Note that between each sample injection for LC−ESI-MS a blank injection was performed to ensure there was no carryover from the previous sample. We estimated the fraction fully exchanged in 3 min for every peptide (Table S1a of the Supporting Information, with averages for overlapping peptides listed in Table S1b of the Supporting Information) as follows. Very large (90−100%) and small (<20%) fractions were estimated visually. Other cases were estimated by fitting the intensities of the two isotopic distributions to two Gaussian curves and using the two resulting areas to compute the fully exchanged fraction. The estimated fractions fully exchanged at 3 min (Table S1b of the Supporting Information) are represented by the colors of the CF monomer peptides and structure in Figure 2. In addition to the peptides of the N- and C-termini discussed above that fully exchange in 3 min, most of the peptides on the C-terminal side of the methylation subdomain (orange) have a 50−64% fraction that fully exchanges in 3 min, but only in the high-density state. A fully exchanged fraction that increases with time would suggest EX1 exchange, in which each opening of the protein to an exchange-competent state is long enough for complete exchange of protons to deuterium.[35] The fully exchanged fraction of the methylation subdomain peptides highlighted in orange does not increase significantly at subsequent early time points (only 3−11% increase at 7, 10, and 15 min), indicating that this rapid exchange (which could be EX1 or EX2) is essentially complete in the 3 min dead time of our experiment. At long times, the m/z cluster for the gradually exchanging fraction merges with that of the fully exchanged fraction.

A qualitative comparison of the mass spectra for two peptides in both states (Figure 4, top) shows that the fraction of the sample with a measurable exchange rate exhibits significantly slower exchange in the kinase-activating state than in the kinase-inhibited state (arrows). The average mass of the isotopic profiles could not be used for this analysis, because it includes the contribution of the rapidly exchanging fraction. Therefore, exchange was quantified by following the mass of the most intense peak in the cluster (neglecting the cluster of the rapidly exchanging fraction). These data are plotted in Figure 4 (bottom), which clearly demonstrates that peptides 473−488 (A, bright orange on the structure) and 500−512 (B, pale orange on the structure) undergo faster exchange in the low-density kinase-inhibited state. Biexponential fits to the data are also shown in the plots, and the resulting parameters for these fits and those for all of the other peptides are listed in Table S3 of the Supporting Information (fractions f_1 and f_2 with rates k_1 and k_2, respectively). Five peptides from the methylation subdomain (rows shaded in orange in Table S3 of the Supporting Information, average peptide length of 12 residues) show significantly faster exchange in the low-density kinase-inhibited state: the weighted average exchange rate constants, computed as $k = (f_1k_1 + f_2k_2)/(f_1 + f_2)$, range from 2.6- to 5.5-fold faster, with the average being 3.8-fold faster. Omitting peptide 473−488 (which is only 2.6-fold faster and is the only peptide that includes residues 473−477) brings the average to 4-fold faster for the regions of residues 478−488 and 499−512. It is not clear why the behavior of the intervening 489−506 peptide exhibits different exchange (Figure S2F of the Supporting Information): both signaling states have an ≈30% rapidly exchanging fraction, and the remaining fraction has a comparable exchange rate in both signaling states. With this one exception, peptides of the C-terminal side of the methylation subdomain (the N-terminal side peptides exchange too quickly to measure) exhibit two changes in the high-density kinase-activating state relative to the low-density kinase-inhibited state: approximately half of the CF exhibits much faster exchange (complete in 3 min), and the other half exhibits 4-fold slower exchange.

The Signaling Subdomain Shows Differential Protection from Exchange with the Signaling State. Peptides from the signaling subdomain that binds CheA and CheW in functional complexes show different degrees of protection from exchange at long times in the high- and low-density signaling states. The three peptides that include the membrane-distal tip of the receptor (spanning residues 377−432) show similar exchange rates in both states, which is evident qualitatively in the series of mass spectra shown in panels A (residues 377−393) and B (residues 381−432) of Figure 5. Furthermore, the plotted data (Figure 5A,B, bottom) have a similar slope, and

dx.doi.org/10.1021/bi500657v | *Biochemistry* 2014, 53, 7755−7764

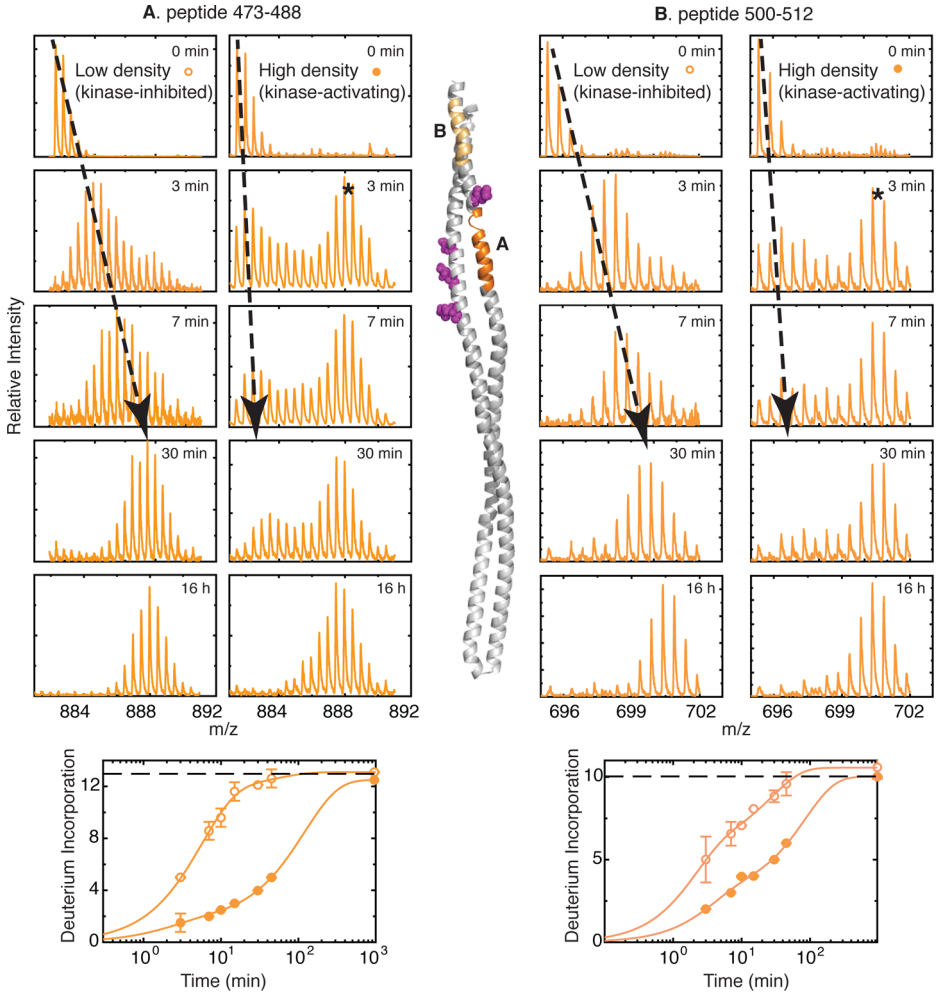

Figure 4. Hydrogen exchange rates change with signaling state in the methylation subdomain. Mass spectra vs exchange time (top) and plots of deuterium incorporation time course (bottom) for two representative peptides of the methylation subdomain, (A) residues 473−488 (bright orange on the structure) and (B) residues 500−512 (pale orange on the structure). For both peptides, in the high-density kinase-activating state, a large fraction undergoes complete exchange in 3 min (asterisks, 64% in part A and 50% in part B). The negligible increase in this fully exchanged fraction in subsequent time points indicates that it is not an EX1 process occurring during the measured time course. The remaining fraction exchanges more slowly in the kinase-activating state than in the kinase-inhibited state (black dashed arrows), and this exchange is quantified in the plots based on the most intense peak in the isotopic cluster (ignoring the rapidly exchanging fraction). The deuterium incorporation plots (bottom) show faster exchange in the kinase-inhibited state (empty circles) than in the kinase-activating state (filled circles). Data plotted are the means ± the standard deviation of two independent experiments; the dashed line represents complete exchange, and parameters resulting from the biexponential fits (lines) are reported in Table S3 of the Supporting Information. Three other peptides (residues 478−488, 479−488, and 499−512) show similar exchange.

the weighted average exchange rate constants are within 30% of each other. However, there is a clear difference in the extent of exchange. Maximal exchange (black mass spectra) is determined using a CF_{4E} sample denatured in D_2O at high temperatures, refolded upon cooling, and subjected to the equivalent protocol so that it undergoes the same degree of back exchange as experimental samples. Both signaling states of these peptides show incomplete exchange at 16 h, and the number of unexchanged protons (protected protons) is greater in the kinase-activating state. As listed in Table S4 of the Supporting Information, all three peptides from this region exhibit a small degree of protection in the low-density kinase-inhibited state (one to two protons) that is significantly larger (five to eight protons) in the high-density kinase-activating state.

Although the majority of the protected sites (five protons) occur in the smallest peptide from the cytoplasmic tip of the receptor within the signaling subdomain, the other two much longer peptides that extend farther into and beyond the signaling subdomain (see Figure 2) show additional protection of two to three protons. These additional protons may be within the signaling subdomain or may be in the adjacent coupling subdomain (C-terminal side). Interestingly, only one other peptide, from the opposite N-terminal side of the coupling subdomain [residues 327−362 (Figure S2B of the Supporting Information)], shows minor protection (two to four protons) from exchange at 16 h.

DISCUSSION

Changes in dynamics in the cytoplasmic domain of bacterial chemoreceptors have long been suggested to be important in the signaling mechanism.[2−7] Previously, disulfide cross-linking has been used as a measure of signaling-related changes in dynamics in the intact receptor in the absence of CheA and

dx.doi.org/10.1021/bi500657v | Biochemistry 2014, 53, 7755−7764

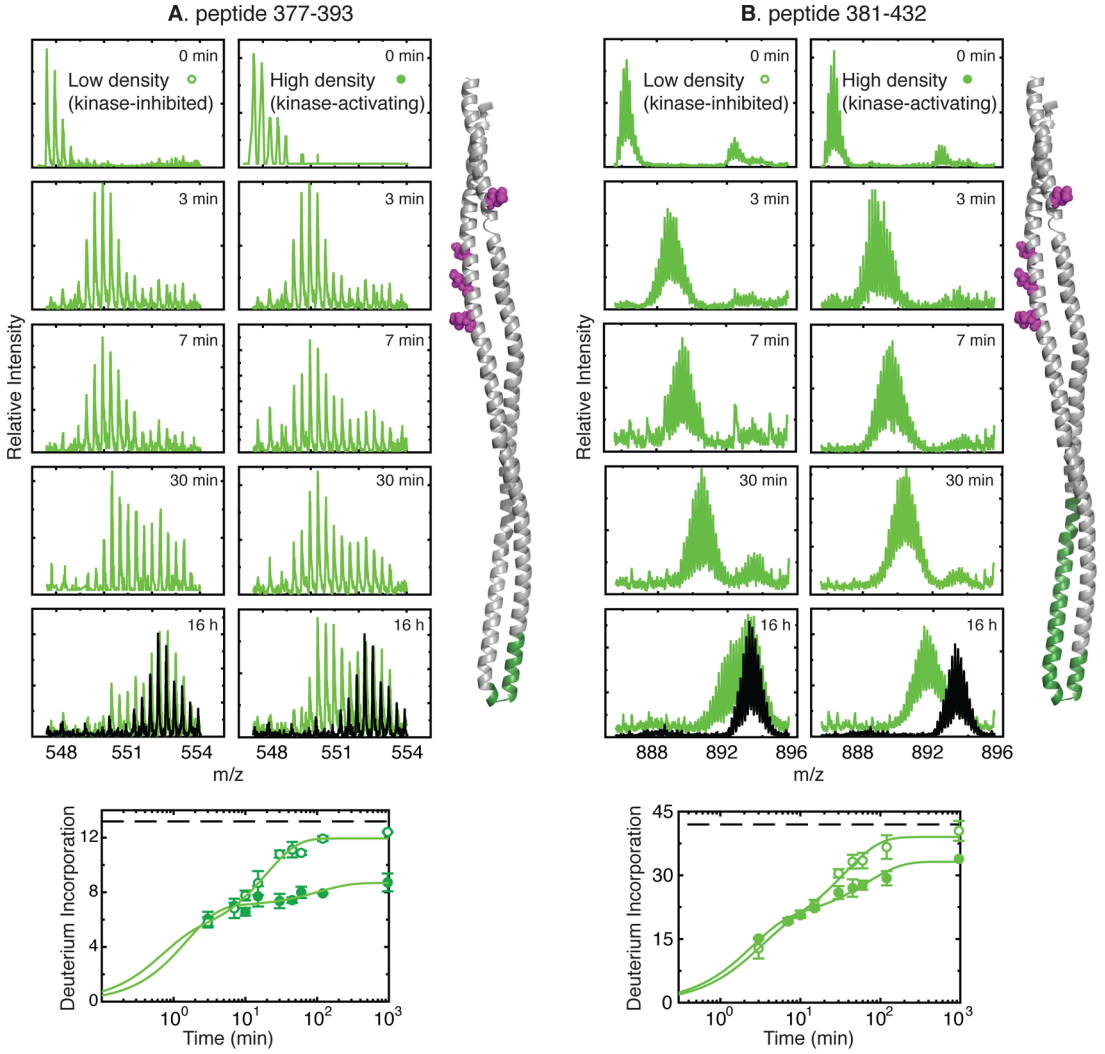

Figure 5. Protection from hydrogen exchange changes with signaling state in the signaling subdomain. Mass spectra vs exchange time (top) and plots of deuterium incorporation time course (bottom) for two representative peptides of the signaling subdomain, (A) residues 377−393 and (B) residues 381−432 (each colored green on the adjacent structure; peptide 384−432 shows similar behavior). Incomplete exchange at the longest time point is shown by the overlay with mass spectra of the maximally exchanged peptide (black), which is the D_2O-denatured control subjected to back exchange after quenching. For the plots, exchange data are quantified on the basis of the average mass over the full range, and biexponential fits (lines) show less protection from exchange at long times in the kinase-inhibited state (empty circles) than in the kinase-activating state (filled circles). Data plotted are the means ± the standard deviation of two independent experiments; the dashed line represents complete exchange, and parameters resulting from the fits are listed in Table S3 of the Supporting Information. The number of hydrogens remaining in all three peptides at 16 h (Table S4 of the Supporting Information) demonstrates consistently greater protection in the high-density kinase-activating state.

CheW.[5] Here we report the first measurements of signaling-related changes in dynamics in functional complexes of the receptor CF, CheA, and CheW, using a new approach[17] that couples vesicle template assembly[18] with HDX-MS. Our measurements demonstrate differences in exchange rates between signaling states that localize to functionally important regions of the chemoreceptor CF involved in excitation and adaptation mechanisms of chemotaxis. These results begin to provide a direct test of proposed models for the role of dynamics in transmembrane signaling and a promising approach for understanding how multiprotein complexes operate in the cell.

Global exchange measurements with this approach have demonstrated significantly slower hydrogen exchange of the entire CF in membrane-bound functional complexes relative to CF alone in solution.[17] We have now used local exchange measurements (localized to pepsin peptides after exchange) to show that this slower exchange occurs throughout the protein. The rapid global exchange of CF alone (~75% exchange at 3 min)[17] is slower in CF complexes in all regions other than the N- and C-termini [~30−70% exchange at 3 min (Table S2 of the Supporting Information)]. The rapid exchange of the C-terminal region (red peptides in Figure 2) is consistent with EPR evidence that this region (beginning at residue 520) is unstructured[34] and serves as a flexible tether to the C-terminal pentapeptide that binds the CheR methyltransferase for modification of the methylation sites.[36] The other rapidly exchanging region at the N-terminus may be due to the absence of the HAMP domain in this construct. The slower exchange measured throughout most of the CF in functional complexes makes it possible to compare the properties of signaling states. The primary differences in dynamics between the high-density CF_{4E} kinase-activating complexes and low-density CF_{4E} kinase-inhibited complexes occur in the methylation and signaling

dx.doi.org/10.1021/bi500657v | *Biochemistry* 2014, 53, 7755−7764

subdomains of the cytoplasmic domain, as represented by the orange and green colors, respectively, of the CF in the model of CF complexes shown in Figure 1A.

Mass spectra and deuterium incorporation plots for representative peptides throughout the rest of the CF show that only small changes are observed between signaling states in other regions (Figure S2 of the Supporting Information). For instance, the high-density state exhibits slightly faster exchange for the early time points in several peptides in the range of residues 422−472 immediately preceding the C-terminal methylation peptides, but no evidence of a subpopulation with complete exchange at 3 min (Figure S2C,E of the Supporting Information). Together with the rapidly exchanging subpopulation of the C-terminal methylation peptides, this accounts for the red region in the 3 min difference exchange map shown in Figure 3. Furthermore, only one peptide outside of the signaling subdomain exhibits protection at long exchange times (Figure S2B of the Supporting Information), and its maximal protection of four protons is more limited than the protection observed in signaling subdomain peptides [maximal protection of eight protons (Table S4 of the Supporting Information)]. Because differences in hydrogen exchange between signaling states are much smaller in these other regions, we have focused our interpretation of this initial study on the changes in exchange in the methylation and signaling subdomain peptides, as illustrated in Figures 4 and 5.

Hydrogen exchange results for the signaling subdomain (Figure 5) indicate that interactions of this subdomain protect a core of protons from exchange at long times (16 h) in both states, and that this protected core is larger in the high-density kinase-activating state. This protection could indicate that this subdomain contains the most stable part of the CF and that it is further stabilized in the kinase-activating state. However, previous studies suggest the opposite occurs during signaling: mutations expected to weaken receptor helix packing in the signaling subdomain have been shown to favor the kinase-activating state.[6] Therefore, we propose this protection is due to interactions with CheA and/or CheW, and that the interaction interface is tighter and/or larger in the kinase-activating state, leading to protection of more protons from exchange. Although the difference in protection could also be due to a differential loss of bound CheA and CheW from the high- and low-density complexes, sedimentation analysis (Figure S1 of the Supporting Information) suggests that the complexes retain equivalent amounts of CheA at 16 h. We suggest that receptors in the kinase-activating state bind tightly to CheA and CheW and loosely to each other, and the opposite occurs in the kinase-inhibited state. Unfortunately, it is not possible to gain insight into the effect of CheA and CheW binding on hydrogen exchange by performing HDX-MS experiments in their absence, because assembly in the absence of CheA and CheW leads to vesicle aggregation.[24]

The methylation subdomain shows both increased and decreased hydrogen exchange rates for most of the C-terminal peptides in the high-density kinase-activating state (Figure 4). Because this heterogeneous behavior (two fractions with different exchange behavior) occurs only in the methylation subdomain peptides, it is not likely to be due to heterogeneity of the CF complexes (e.g., native vs denatured or complexed with CheA and CheW vs uncomplexed), which would be expected to alter exchange of the entire CF. Instead, it is interesting to consider the possibility that the C-terminal methylation subdomain of each monomer in the CF dimer experiences a different environment, consistent with the ≈60/40 fractions observed to have different exchange behavior. For instance, if the methylation subdomain is contracted in the kinase-activating state, such that the CF occupies a smaller area of the membrane, this could increase the level of interaction between the CF monomers with the closest C-terminal helices in the methylation subdomain within the trimer of dimers, leading to a decreased exchange rate. This could leave the other monomer more solvent-exposed and undergoing very rapid exchange, comparable to the rapid exchange of the N-terminal peptides of the methylation subdomain. The decrease in exchange rate observed in the methylation subdomain peptides for the other 40% fraction of the CF may be due to stabilization of this subdomain in the kinase-activating state, which would be consistent with proposals from the laboratories of Falke and Parkinson.[6,7] However, because of the complex HDX behavior of these peptides, which is likely to be influenced by multiple factors (see below), it is too early to conclude whether this subdomain is stabilized in the kinase-activating state.

Limitations of this initial study of exchange properties of CF4E in functional complexes include the possibility that low- versus high-density assembly rather than signaling-state differences causes some of the observed changes in HDX. Results of preliminary experiments on low-density CF4Q complexes (data not shown), which are kinase-on but have kinase activity lower than that of high-density CF4E, indicate that the two detected signaling subdomain peptides (381−432 and 384−432) show protection from exchange at 16 h comparable to that of the kinase-on high-density CF4E. This suggests that the HDX differences we report in the signaling subdomain are not due to low- versus high-density assembly differences and may be due to the signaling state. On the other hand, the HDX behavior of the methylation subdomain peptides of low-density CF4Q is complex, seemingly intermediate between the properties of high-density CF4E and low-density CF4E. Thus, it appears that multiple factors (density of assembly, methylation state, and kinase activity) influence the complex HDX properties in the methylation subdomain.

HDX-MS of CF4E complexes with high and low kinase activity modulated by density of assembly reveals that changes localize to the functionally important methylation and signaling subdomains, as represented by the CF colors in the structural model of Figure 1A. Experiments are in progress to further optimize vesicle-assembled samples and then compare HDX of a variety of CF complexes using other means such as mutations and methylation state to alter the kinase activity. These comparisons will reveal which changes in HDX properties correlate with signaling state and will test models for changes in dynamics of CF subdomains during signaling.

Measurements of hydrogen exchange of subdomains of a protein within functional complexes can provide insight into mechanistically important changes in both conformation (exchange rates may decrease because of a decreased level of solvent exposure) and dynamics (exchange rates may decrease because of a decreased number of conformational fluctuations or increased stability). The results of this initial study of exchange in functional CF complexes suggest changes in both conformation and stability. In the methylation subdomain, we suggest that one monomer is rapidly exchanging because of increased solvent exposure and/or instability and the other monomer is stabilized by closer interactions within the trimer of dimers. In the signaling subdomain, we suggest that a larger or more stable interaction with CheA and/or CheW reduces

exchange at long times. Future measurements will seek to determine which observed differences in exchange best correlate with signaling states and to determine the underlying cause of these differences.

HDX-MS, an important approach for characterizing the mechanistic role of protein dynamics, has been applied in a few other cases to multiprotein complexes.[10,11,37] The combination of vesicle template assembly with HDX-MS that we have used for measurements of local exchange in nativelike chemoreceptor complexes should be applicable to a wide variety of functional complexes formed by membrane proteins. Indeed, vesicle template assembly has been successful for assembly of functional complexes of cytoplasmic domains of other membrane proteins such as receptor kinases.[20−23] This provides a promising approach for measuring functionally important dynamics to advance our understanding of mechanisms of membrane proteins and their complexes.

■ ASSOCIATED CONTENT

Supporting Information

Rapidly exchanging fractions (Table S1), the time course of deuterium incorporation (Table S2), hydrogen exchange rates and protection factors for both high- and low-density states (Table S3), numbers of protons protected from exchange at long times in signaling subdomain peptides (Table S4), sedimentation analysis of binding of CheA to complexes (Figure S1), and mass spectra and plots of exchange for representative peptides throughout the CF (Figure S2). This material is available free of charge via the Internet at http://pubs.acs.org.

■ AUTHOR INFORMATION

Corresponding Author

*Department of Chemistry, 122 LGRT, 710 N. Pleasant St., University of Massachusetts, Amherst, MA 01003. E-mail: thompson@chem.umass.edu. Telephone: (413) 545-0827.

Funding

This research was supported by National Institutes of Health Grant R01-GM085288. S.S.K. was partially supported by a fellowship from the University of Massachusetts as part of the Chemistry-Biology Interface Training Program (National Research Service Award T32 GM08515).

Notes

The authors declare no competing financial interest.

[‖]Deceased.

■ ACKNOWLEDGMENTS

We thank Cedric Bobst, Guanbo Wang, Shunhai Wang, Serap Pektas, and Cristina Martin for mass spectrometry advice and technical assistance, Daniel Fowler and Yuzhou Tang for providing some CheA and CheW proteins, past and present members of the Thompson and Weis groups for helpful discussions, and Sandy Parkinson and Rick Dahlquist for helpful comments on the manuscript.

■ ABBREVIATIONS

CF, cytoplasmic fragment of *Escherichia coli* aspartate chemotaxis receptor; DGS-NTA, 1,2-dioleoyl-*sn*-glycero-3-[*N*-(5-amino-1-carboxypentyl)iminodiacetic acid] (Ni-chelating lipid); DMSO, dimethyl sulfoxide; DOPC, 1,2-dioleoyl-*sn*-glycero-3-phosphocholine; GuHCl, guanidine hydrochloride; HAMP, histidine kinases, adenyl cyclases, MCPs, and some phosphatases; HDX-MS, hydrogen−deuterium exchange mass spectrometry; HPLC, high-pressure liquid chromatography; LC−ESI-MS, liquid chromatography and electrospray ionization mass spectrometry; TCEP, tris(2-carboxyethyl)phosphine.

■ REFERENCES

(1) Falke, J. J., and Hazelbauer, G. L. (2001) Transmembrane signaling in bacterial chemoreceptors. *Trends Biochem. Sci. 26*, 257−265.

(2) Seeley, S. K., Weis, R. M., and Thompson, L. K. (1996) The cytoplasmic fragment of the aspartate receptor displays globally dynamic behavior. *Biochemistry 35*, 5199−5206.

(3) Murphy, O. J., Yi, X., Weis, R. M., and Thompson, L. K. (2001) Hydrogen Exchange Reveals a Stable and Expandable Core within the Aspartate Receptor Cytoplasmic Domain. *J. Biol. Chem. 276*, 43262−43269.

(4) Kim, S.-H., Wang, W., and Kim, K. K. (2002) Dynamic and clustering model of bacterial chemotaxis receptors: Structural basis for signaling and high sensitivity. *Proc. Natl. Acad. Sci. U.S.A. 99*, 11611−11615.

(5) Starrett, D. J., and Falke, J. J. (2005) Adaptation Mechanism of the Aspartate Receptor: Electrostatics of the Adaptation Subdomain Play a Key Role in Modulating Kinase Activity. *Biochemistry 44*, 1550−1560.

(6) Swain, K. E., Gonzalez, M. A., and Falke, J. J. (2009) Engineered Socket Study of Signaling through a Four-Helix Bundle: Evidence for a Yin−Yang Mechanism in the Kinase Control Module of the Aspartate Receptor. *Biochemistry 48*, 9266−9277.

(7) Zhou, Q., Ames, P., and Parkinson, J. S. (2009) Mutational analyses of HAMP helices suggest a dynamic bundle model of input-output signalling in chemoreceptors. *Mol. Microbiol. 73*, 801−814.

(8) Barrera, N. P., and Robinson, C. V. (2011) Advances in the mass spectrometry of membrane proteins: From individual proteins to intact complexes. *Annu. Rev. Biochem. 80*, 247−271.

(9) Laganowsky, A., Reading, E., Hopper, J. T. S., and Robinson, C. V. (2013) Mass spectrometry of intact membrane protein complexes. *Nat. Protoc. 8*, 639−651.

(10) Busenlehner, L. S., Brändén, G., Namslauer, I., Brzezinski, P., and Armstrong, R. N. (2008) Structural elements involved in proton translocation by cytochrome c oxidase as revealed by backbone amide hydrogen-deuterium exchange of the E286H mutant. *Biochemistry 47*, 73−83.

(11) Orban, T., Jastrzebska, B., Gupta, S., Wang, B., Miyagi, M., Chance, M. R., and Palczewski, K. (2012) Conformational dynamics of activation for the pentameric complex of dimeric G protein-coupled receptor and heterotrimeric G protein. *Structure 20*, 826−840.

(12) West, G. M., Chien, E. Y. T., Katritch, V., Gatchalian, J., Chalmers, M. J., Stevens, R. C., and Griffin, P. R. (2011) Ligand-dependent perturbation of the conformational ensemble for the GPCR β2 adrenergic receptor revealed by HDX. *Structure 19*, 1424−1432.

(13) Chung, K. Y., Rasmussen, S. G. F., Liu, T., Li, S., DeVree, B. T., Chae, P. S., Calinski, D., Kobilka, B. K., Woods, V. L., and Sunahara, R. K. (2011) Conformational changes in the G protein Gs induced by the β2 adrenergic receptor. *Nature 477*, 611−615.

(14) Rey, M., Man, P., Clémençon, B., Trézéguet, V., Brandolin, G., Forest, E., and Pelosi, L. (2010) Conformational dynamics of the bovine mitochondrial ADP/ATP carrier isoform 1 revealed by hydrogen/deuterium exchange coupled to mass spectrometry. *J. Biol. Chem. 285*, 34981−34990.

(15) Mehmood, S., Domene, C., Forest, E., and Jault, J.-M. (2012) Dynamics of a bacterial multidrug ABC transporter in the inward- and outward-facing conformations. *Proc. Natl. Acad. Sci. U.S.A. 109*, 10832−10836.

(16) Hebling, C. M., Morgan, C. R., Stafford, D. W., Jorgenson, J. W., Rand, K. D., and Engen, J. R. (2010) Conformational analysis of membrane proteins in phospholipid bilayer nanodiscs by hydrogen exchange mass spectrometry. *Anal. Chem. 82*, 5415−5419.

(17) Koshy, S. S., Eyles, S. J., Weis, R. M., and Thompson, L. K. (2013) Hydrogen Exchange Mass Spectrometry of Functional Membrane-Bound Chemotaxis Receptor Complexes. *Biochemistry 52*, 8833−8842.
(18) Shrout, A. L., Montefusco, D. J., and Weis, R. M. (2003) Template-Directed Assembly of Receptor Signaling Complexes. *Biochemistry 42*, 13379−13385.
(19) Besschetnova, T. Y., Montefusco, D. J., Asinas, A. E., Shrout, A. L., Antommattei, F. M., and Weis, R. M. (2008) Receptor density balances signal stimulation and attenuation in membrane-assembled complexes of bacterial chemotaxis signaling proteins. *Proc. Natl. Acad. Sci. U.S.A. 105*, 12289−12294.
(20) Zhang, X., Gureasko, J., Shen, K., Cole, P. A., and Kuriyan, J. (2006) An allosteric mechanism for activation of the kinase domain of epidermal growth factor receptor. *Cell 125*, 1137−1149.
(21) Shrout, A. L., Esposito, E. A., and Weis, R. M. (2008) Template-directed Assembly of Signaling Proteins: A Novel Drug Screening and Research Tool. *Chem. Biol. Drug Des. 71*, 278−281.
(22) Esposito, E. A., Shrout, A. L., and Weis, R. M. (2008) Template-Directed Self-Assembly Enhances RTK Catalytic Domain Function. *J. Biomol. Screening 13*, 810−816.
(23) Shi, F., Telesco, S. E., Liu, Y., Radhakrishnan, R., and Lemmon, M. A. (2010) ErbB3/HER3 intracellular domain is competent to bind ATP and catalyze autophosphorylation. *Proc. Natl. Acad. Sci. U.S.A. 107*, 7692−7697.
(24) Montefusco, D. J., Shrout, A. L., Besschetnova, T. Y., and Weis, R. M. (2007) Formation and Activity of Template-Assembled Receptor Signaling Complexes. *Langmuir 23*, 3280−3289.
(25) Briegel, A., Wong, M. L., Hodges, H. L., Oikonomou, C. M., Piasta, K. N., Harris, M. J., Fowler, D. J., Thompson, L. K., Falke, J. J., Kiessling, L. L., and Jensen, G. J. (2014) New insights into bacterial chemoreceptor array structure and assembly from electron cryotomography. *Biochemistry 53*, 1575−1585.
(26) Asinas, A. E., and Weis, R. M. (2006) Competitive and cooperative interactions in receptor signaling complexes. *J. Biol. Chem. 281*, 30512−30523.
(27) Kott, L., Braswell, E. H., Shrout, A. L., and Weis, R. M. (2004) Distributed subunit interactions in CheA contribute to dimer stability: A sedimentation equilibrium study. *Biochim. Biophys. Acta 1696*, 131−140.
(28) Fowler, D. J., Weis, R. M., and Thompson, L. K. (2010) Kinase-active Signaling Complexes of Bacterial Chemoreceptors Do Not Contain Proposed Receptor−Receptor Contacts Observed in Crystal Structures. *Biochemistry 49*, 1425−1434.
(29) Fang, J., Rand, K. D., Beuning, P. J., and Engen, J. R. (2011) False EX1 signatures caused by sample carryover during HX MS analyses. *Int. J. Mass Spectrom. 302*, 19−25.
(30) Briegel, A., Beeby, M., Thanbichler, M., and Jensen, G. J. (2011) Activated chemoreceptor arrays remain intact and hexagonally packed. *Mol. Microbiol. 82*, 748−757.
(31) Sferdean, F. C., Weis, R. M., and Thompson, L. K. (2012) Ligand affinity and kinase activity are independent of bacterial chemotaxis receptor concentration: Insight into signaling mechanisms. *Biochemistry 51*, 6920−6931.
(32) Vaknin, A., and Berg, H. C. (2007) Physical Responses of Bacterial Chemoreceptors. *J. Mol. Biol. 366*, 1416−1423.
(33) Briegel, A., Ames, P., Gumbart, J. C., Oikonomou, C. M., Parkinson, J. S., and Jensen, G. J. (2013) The mobility of two kinase domains in the *Escherichia coli* chemoreceptor array varies with signalling state. *Mol. Microbiol. 89*, 831−841.
(34) Bartelli, N. L., and Hazelbauer, G. L. (2011) Direct evidence that the carboxyl-terminal sequence of a bacterial chemoreceptor is an unstructured linker and enzyme tether. *Protein Sci. 20*, 1856−1866.
(35) Eyles, S. J., and Kaltashov, I. A. (2004) Methods to study protein dynamics and folding by mass spectrometry. *Methods 34*, 88−99.
(36) Wu, J., Li, J., Li, G., Long, D. G., and Weis, R. M. (1996) The receptor binding site for the methyltransferase of bacterial chemotaxis is distinct from the sites of methylation. *Biochemistry 35*, 4984−4993.
(37) Xiao, H., Wang, H., Zhang, X., Tu, Z., Bulinski, C., Khrapunovich-Baine, M., Hogue Angeletti, R., and Horwitz, S. B. (2012) Structural evidence for cooperative microtubule stabilization by Taxol and the endogenous dynamics regulator MAP4. *ACS Chem. Biol. 7*, 744−752.